The Effect of a Temperature-dependent Permeability Limit on the Convective Upflow and Temperature in a Numerically Modelled Geothermal System

Dona Banerjee[1], David Dempsey[1], Dale Cusack[1], James Hewett[1], Ben Kennedy[1], and John Cater[1]

[1]University of Canterbury, 20 Kirkwood Avenue, Upper Riccarton, Christchurch 8041, New Zealand

dona.banerjee@canterbury.ac.nz

Keywords: *Brittle-ductile, flow, temperature-dependent permeability, convection, geothermal*

ABSTRACT

High-temperature (>220 °C) geothermal fields within the Taupō Volcanic zone (TVZ) are among the most promising resources for clean energy production and present a significant opportunity for sustainable energy development. An emerging frontier is the exploitation of geothermal fluids at superhot or supercritical temperatures higher than 350°C.

In this work, numerical simulations of geothermal convection cells are used to investigate how thermal and physical rock properties influence heat transfer and geothermal accessibility at supercritical conditions. The focus of this work is the influence of thermally controlled brittle-ductile transition on the permeability properties of rock, that reduces fluid transport below a threshold temperature value.

A range of convection cell scenarios has been investigated with varying circulation depth, Brittle-Ductile Transition (BDT) temperature range, and permeability anisotropy. For a BDT across the range 340 to 440°C, the estimated temperatures in convection cells at a depth of 2 km exceeded the highest recorded TVZ temperatures (340°C). As flow was permitted at progressively higher temperatures, shallow temperatures reached those consistent with supercritical wells in Krafla, Iceland.

These preliminary results suggest that, to be consistent with New Zealand geothermal characteristics, heat transfer is likely to be conduction-dominated at supercritical temperatures and depths. However, future analysis of alternative mechanisms of permeability creation and loss, improved descriptions of temperature varying fluid properties, and better models of shallow permeability under transient simulations may require that we revisit this finding.

1. INTRODUCTION

The Taupō Volcanic Zone (TVZ) of New Zealand's central North Island hosts multiple high-enthalpy geothermal fields. These fields are the upper depths of a larger upflow system that transport magmatic heat through the rifting crust (Rowland et al., 2010). Some of these fields have been developed for electricity production (Fig. 1), sourcing hot water between depths of 1-3 km. Other fields hold protected status and are not available for power production.

The assemblage of geothermal systems is a large-scale manifestation of Rayleigh-Benard convection (Couston et al., 2022). Multiple circulation cells form above a hot rock layer, with broad distributed downwelling of cold water from the surface (mostly meteoric rainwater) and discrete localised upflows of hot, lower density water (McNabb, 1975; Weir, 2009; Dempsey et al., 2012a). These individual upflows have estimated power availability of hundreds of megawatts (Bibby et al., 1995; Weir, 2009). The circulation is assumed to be confined to the brittle crust, estimated to extend to a depth of between 6 to 8 km, based on the distribution of shallow seismicity (Bryan et al., 1999). Temperatures of individual geothermal fields vary but have been known to reach 340°C in Rotokawa (Sewell et al., 2015; McNamara et al., 2016).

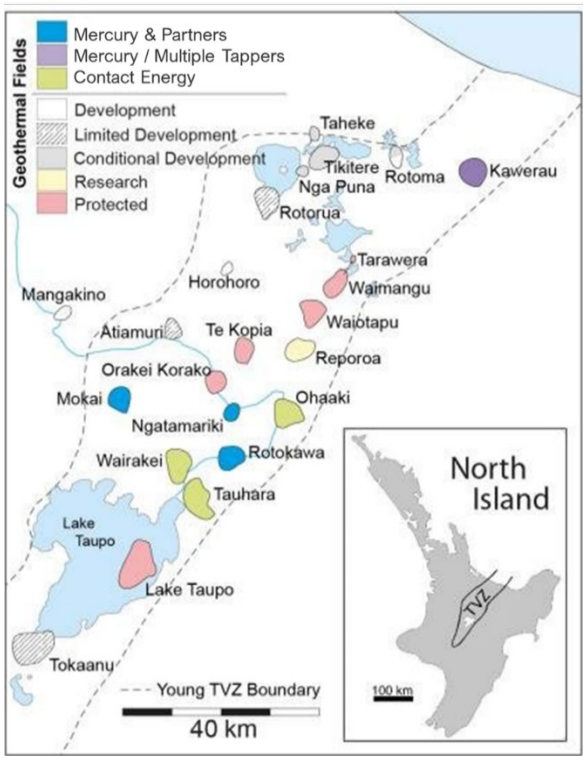

Figure 1: Geothermal fields of the Taupō Volcanic Zone (Wilson et al., 1995), shown by their resistivity boundaries (Bibby et al., 1995).

In hydrothermal systems outside New Zealand, flowing temperatures above 400°C have sometimes been observed. Examples include an IDDP (Iceland Deep Drilling Project) well in Iceland that encountered magma in the Krafla system (450°C) and another on the Reykjanes peninsula (426°C; Friðleifsson et al., 2020). Temperatures as high as 500°C have been encountered in the Kakkonda geothermal system (Japan)

ISSN 2703-4275

and Larderello (Italy), although in both cases the permeability was below the threshold for convection (Ikeuchi et al., 1998; Margo et al., 2019).

The permeability of rock describes how rapidly water flows through it with an applied pressure gradient. Understanding what controls permeability is important for understanding the deep circulation in geothermal systems. For instance, there is a minimum permeability needed to sustain convection – this threshold is likely to be around 10^{-16} m^2 at temperatures of ~350°C (Hanano, 2004). At permeabilities below this value, water moves too slowly to contribute appreciably to heat transport. Instead, conduction dominates, which is a relatively inefficient mechanism for heat transfer.

A simplistic characterisation of the thermal behaviour of rock is that it transitions from predominantly brittle to dominantly ductile behaviour across a defined temperature range. For quartzofeldspathic rocks, this transition is commonly assumed to occur between 350 and 400°C (Scholz, 1988; Fournier, 1999). Above this range, high temperature and pressure contribute to reorganisation of the rock structure through grain-mineral reorientation towards a more compact, less porous and less permeable mass. However, recent laboratory experiments (Watanabe et al., 2017; Meyer et al., 2024) have suggested that meshes of microfractures may develop and persist within the ductile regime, although the measured permeabilities of these meshes were typically below convective thresholds. Rock type is also important; some basaltic rock types may be more resistant to thermally induced ductility and have a higher transition temperature (Violay et al., 2012).

Permeability is also influenced by confining pressure, porosity and pore type, the latter of which are controlled by rock type (Villeneuve et al., 2024). The confining pressure at the BDT depth is also sensitive to differential stress and has complex interactions with rock types in hydrothermally altered areas that can locally drive BDT to shallow 1-2km depth (e.g. Mordensky et al., 2019).

The connection between upper crust brittle failure and elevated permeability is well-established (Manning and Ingebritsen, 1999; Townend & Zoback, 2000). Nevertheless, in dynamic hydrothermal environments, it is recognised that other mechanisms contribute to permeability loss and renewal across a range of time scales. This includes mineralisation and tectonic or fluid-induced reactivation of fractures (Henneberger & Browne, 1988; Sibson, 1996; Micklethwaite & Cox, 2004; Dempsey et al., 2012b). A complete characterisation of permeability must describe its time-varying characteristics.

It is generally difficult to access and observe rock at high temperatures and below depths of 3 km. Therefore, an understanding of permeability behaviour in hydrothermal systems is sometimes obtained through modelling and inference (Hayba & Ingebritsen, 1997; Scott et al., 2016; Kissling et al., 2024). One way to indirectly estimate the maximum flowing temperature at depth is to observe temperatures in the shallower reaches of geothermal systems. The idea is that if flowing geothermal fluids are sampled in a well at a temperature of, say, 350°C, then those fluids must have at some point encountered rock at least as hot as this. Indeed, the maximum temperature will be higher than observed near the surface when cooling within the upflow is considered (Hayba & Ingebritsen, 1997).

The goal of this study is to test the effect of a thermally induced permeability loss on hydrothermal circulation. It is important to understand how a transition temperature at the deep root of a circulation cell, approximating a brittle-ductile transition, influences shallow fluid temperatures that might be sampled in wells. If a relationship can be established, this would allow the inference of otherwise unobservable constraints on deep circulation from surface measurements. This analysis has been undertaken using numerical models that capture density-driven flow of pure water across crustal depths, incorporating permeability as an explicit function of temperature. These models are intended to test whether the brittle-ductile transition (BDT) zone can help explain the shallow geothermal temperatures observed in New Zealand and elsewhere

2. METHODOLOGY

2.1 Prior models of hydrothermal systems

Previous studies that have examined the impact of deep permeability on the structure of hydrothermal convection can be separated into two types; those that do, and do not include an explicit dependence on temperature. Of the latter, we include studies by Dempsey et al. (2012b) and Kissling et al. (2024) amongst others, whom considered logarithmic, or power-law permeability models inspired by those suggested in Manning & Ingebritsen (1999). In these models, permeability decreases with depth reflecting processes of crack closure or compaction at higher ambient stress. Hydrothermal circulation is typically driven by a basal boundary condition at an elevated temperature, approximating the rifted and heavily intruded midcrust of the TVZ – a hotplate.

A second class of permeability model includes an explicit temperature dependence. These models are typically used for understanding magmatic intrusions and the hydrothermal circulation around them. Studies by Hayba & Ingebritsen (1997) and Scott et al. (2016) used a sigmoidal function to implement a smooth decrease in permeability with rising temperature across a defined transition range. These studies included a discrete magma body at shallow depths that was the primary source of heat driving the evolution of a hydrothermal system.

2.2 Model and mesh structure

Numerical experiments were conducted in COMSOL Multiphysics v6.2, a finite element solver for partial differential equations that supports both steady state and time dependent simulations. It is well-suited to the goals of this study due to its ability to define temperature-dependent properties for both the porous medium and the fluid that flows through it.

The model used included a coupled solution, combining heat and mass transfer, with Darcy's Law for fluid flow and heat transfer (conduction and advection) in porous media. A 2D axisymmetric domain was used to capture a concentrated

Proceedings 47th New Zealand Geothermal Workshop
11 -13 November 2025
Rotorua, New Zealand
ISSN 2703-4275

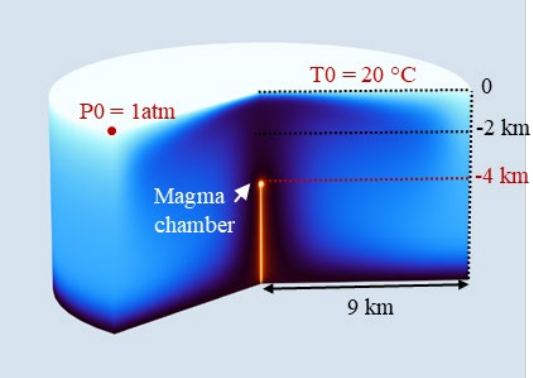

Figure 2: A 2D axisymmetric model showing a conduit leading up to a spherical magma chamber at 4 km depth. Dark to light blue shading shows the steady state temperature distribution result for a typical simulation.

central upflow region (around the model axis) and a more distributed region of downwelling that surrounds it (Fig. 2).

All of the models have a fixed radius of 9 km and a variable depth to a lower hotplate. An idealised magma chamber was also included as a spherical intrusion with a radius of 100 m located at a depth of 4 km. The magma chamber is connected to the hotplate via a narrow conduit. Including both hotplate and magmatic intrusion allows consideration of the relative heat contribution from both sources.

The surface temperature, T0, was fixed to 20 °C and an elevated geothermal gradient of 50 °C/km was used to determine the fixed basal temperature. The depth of the model was varied based on the precise BDT temperature range tested. The magma chamber boundary was fixed at a temperature of 800°C. A pointwise constraint of 1 atm was set at the upper edge of the model to establish a reference pressure in order to obtain a unique solution. Zero mass flow was enforced at all boundaries such that the circulation cells were entirely contained within the domain. This is not a precise representation of a rainfall-fed hydrothermal system, as it assumes continual recycling. However, we do not expect this simplification to affect the conclusions of the study.

A structured mesh (Fig. 3) with refined elements is applied near the magma conduit and chamber to preserve element quality in regions with high thermal gradients and curved geometry. Curved skewness was above 0.49 throughout to aid with numerical stability. Element size ranges from 1 m to 80 m, with element refinement near the curved magma chamber and at the bottom of the central axis to improve convergence where steep gradients are expected. The mesh consists of 54 vertex elements. It also consists of 2164 up to 2434 boundary elements for BDT temperature ranges of 340 to 440°C, up to 520 to 620 °C. Overall, a minimum element quality of 0.4919 was achieved.

The model solutions were used to obtain steady state pressure and temperature distributions. This could generally be achieved for permeability values lower than 10^{-15} m^2. Above this value, non-steady convection may occur. Future work will investigate transient simulations.

For each simulation, several variables were recorded: 1. Temperature: a vertical profile immediately above the magma chamber as well as the maximum temperature obtained at a depth of 2 km (following Kissling et al., 2024).

2. Power: the heat throughput of the upflow was calculated as the integral of heat flux through a radial cross section extending 2 km from the axis and at a depth of 2 km. Conductive heat flows at the hotplate and magma boundaries were also noted.

2.3 Governing equations

The mass conservation equation is

$$\nabla \cdot (\rho \mathbf{u}) = Q_{\mathrm{m}}, \quad (1)$$

where ρ is the temperature-dependent density (described in Section 2.3.1) and Q_{m} is the rate of mass added or removed [kg/m^3· s] from the porous medium. The fluid velocity $\mathbf{u}$ [m/s] is calculated from the pressure field using Darcy's law:

$$\mathbf{u} = \frac{\kappa}{\mu}\nabla(p - \rho g), \quad (2)$$

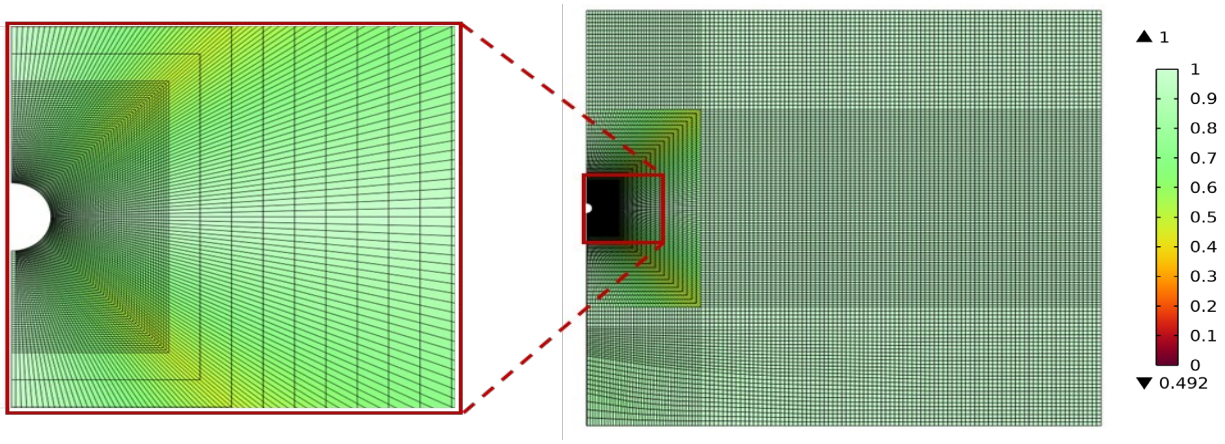

Figure 3: Mesh curve skewness across the model with lefthand zoom showing refinement around the magma chamber.

Proceedings 47th New Zealand Geothermal Workshop
11 -13 November 2025
Rotorua, New Zealand
ISSN 2703-4275

where κ is permeability [m^2], μ is dynamic viscosity of the fluid [Pa·s], p is pressure [Pa], and g is the gravitational acceleration.

The heat transfer equation is:

$$\rho c_p \ \mathbf{u} \cdot \nabla T + \nabla \cdot \mathbf{q} = Q, \qquad (3)$$

where c_p is the specific heat capacity of the fluid [J/(kg·K)], ∇T is the temperature gradient [K/m], $\nabla \cdot \mathbf{q}$ is conduction [W/m^3], and Q includes heat sources [W/m^3]. The advection term is $\mathbf{u} \cdot \nabla T$ and conduction term is $\nabla \cdot \mathbf{q}$, with Fourier's law of conduction computed as:

$$\mathbf{q} = - k_{\text{eff}} \nabla T, \qquad (4)$$

where k_{eff} is the effective thermal conductivity [W/m·K] within the porous media.

2.4 Constitutive material properties

The density of the fluid is expressed as a function of temperature. Ideally, fluid properties would be derived from International Association for the Properties of Water and Steam (IAPWS) formulation, which considers accurate thermophysical properties over a wide range of pressures and temperatures. However, implementing this equation of state in COMSOL was not possible within the scope of this study.

As an alternative, the parameterisation of Weir (2009) was used, which expresses density as a quadratic function of temperature, and is accurate to 1.5% in the range 100-300°C.

$$\rho \ = \ 1000 - 0.0033T^2. \qquad (5)$$

The density function was extended beyond this range and truncated within the impermeable domain where heat advection is negligible (Fig. 4(b)). While this avoids the complexities of multi-phase systems, it does mean that the results may not be strictly applicable to geothermal systems boiling at a depth of 2 km or more. The density approximation is increasingly different to IAPWS values for higher BDT temperatures and the resulting implications are discussed later.

Following Hayba & Ingebritsen (1997), permeability loss with temperature is described by a sigmoid function (Fig. 4a). The key parameters to select are limiting values of permeability, and a midpoint and width of the temperature transition:

$$\log_{10}(\kappa) = \ K_{\max} + \frac{K_{\max} - K_{\min}}{1 + \exp(-(T - T_{\text{mid}})/\Delta T)}, \qquad (6)$$

where $K_{\max}$ and $K_{\min}$ are bounding permeabilities in log-space, T_{mid} [°C] is the mid-point temperature of the brittle-ductile transition zone and ΔT [°C] parameterises the width. Two permeability functions with different BDTs are shown in Fig. 4(a) – these end members model rock that becomes impermeable at low and high temperature limits. As all models considered share the same ΔT of 100°C, different BDT models are distinguished by their midpoint temperature value. For instance, the two models shown in Fig. 4(a) are denoted BDT 390°C and 570°C.

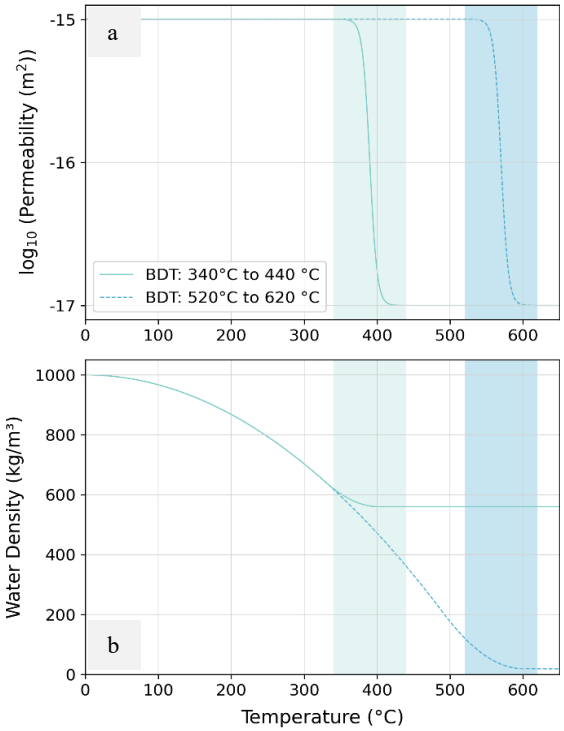

Figure 4: (a) Permeability is represented by a sigmoid function to simulate a gradual and continuous decline in permeability across the BDT zone, avoiding abrupt changes imposed by stepwise or layer-based models. (b) Temperature-dependent water density curve, that is extended up to the full BDT temperature range used.

Conductive and advective heat transport both influence the temperature distribution in the solution. This in turn modifies the local density and permeability values, which in turn causes fluid movement to respond to these changes. The fluid velocity within COMSOL Multiphysics is computed using the *Darcy's Law* module. The *Heat Transfer for porous media* module is used to solve the heat transfer equation. Coupling these two modules enabled the simulation of a fully coupled system, where pressure, temperature, permeability and fluid density alter in response to BDT-related thermal conditions.

3. RESULTS

3.1 Convection cells

Fig. 5 presents typical examples of convection cells. These exhibit a single upflow centred on the domain axis with relatively large upward velocity. Velocities decrease and then reverse to downwelling with increasing radial distance. The highest temperatures occur within the upflow, spreading outward near the surface.

The results show that the high-temperature low permeability region begins at the magma chamber and extends downwards to the hotplate. The thickness of the impermeable zone depends on the onset of permeability loss for the particular parameter values that were used.

Proceedings 47th New Zealand Geothermal Workshop
11 -13 November 2025
Rotorua, New Zealand
ISSN 2703-4275

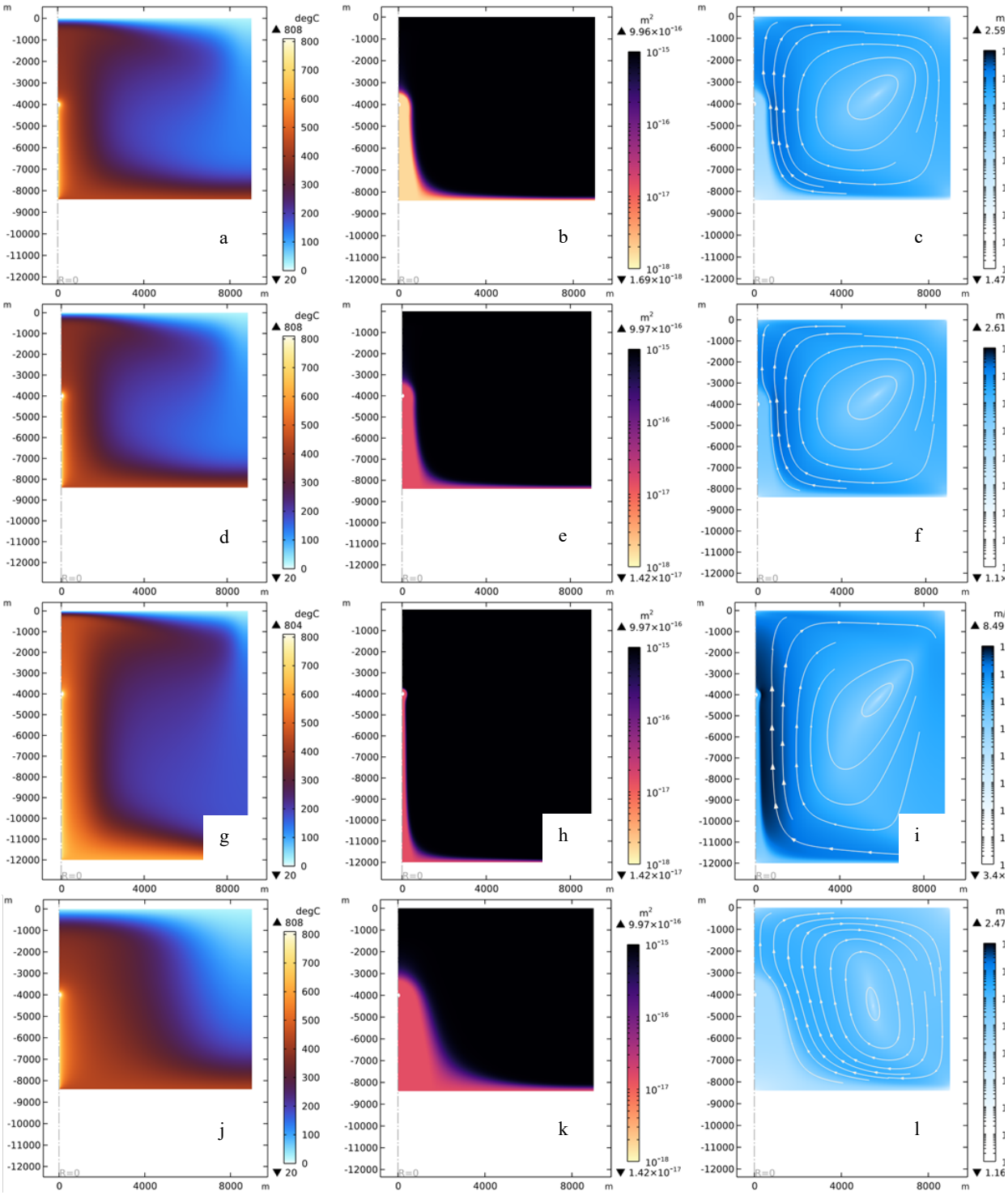

Figure 5: Temperature (°C), permeability (m^2) and velocity magnitudes (m/s) for several indicative scenarios. (a-c) A host rock with a low BDT temperature range from 340 to 440 °C and permeabilities between $1x10^{-15}$ to $1x10^{-18}$ m^2. (d-f) A host rock with a low BDT temperature range from 340 to 440 °C and permeabilities between $1x10^{-15}$ to $1x10^{-17}$ m^2. (g-i) A host rock with a high BDT temperature range from 520 to 620 °C and permeabilities between $1x10^{-15}$ to $1x10^{-17}$ m^2. (j-l) The same host rock as (d-f) but with a vertical permeability reduced by a factor of 10.

5

ISSN 2703-4275

For the low and high BDT temperature ranges of 340-440°C and 520-620°C respectively, shown in Figs. 5(d), 5(g) and 6, the maximum modelled temperatures at 2 km depth were 385°C and 487°C (Fig. 6), respectively. The convective power output of the upflow rises from 124 to 174 MW

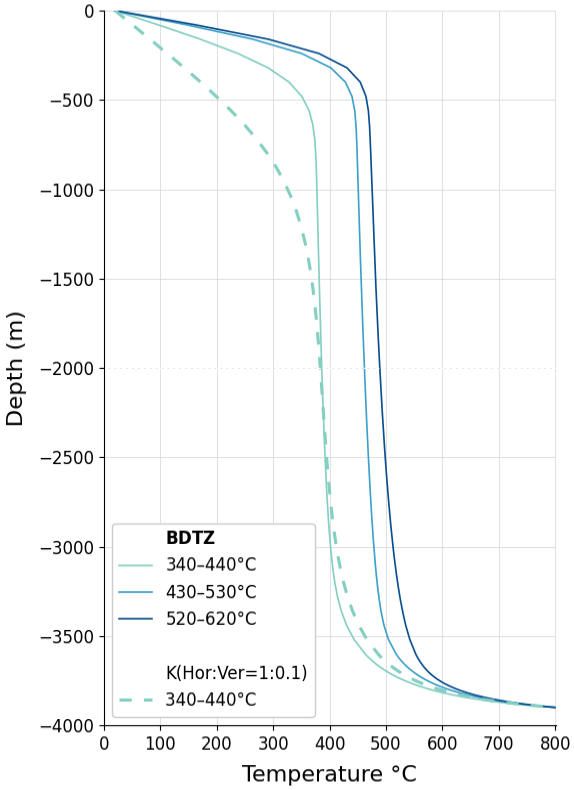

Figure 6: Vertical temperature profiles from surface to the magma body for different BDT ranges.

accordingly.

The model with the higher BDT temperature has a deeper vertical extent, which was found to be necessary for numerical stability. However, sensitivity tests of up to 1 km change in vertical model extent show no influence on the predicted field power output.

The Rayleigh number (Ra) (Kissling, 2004) provides a criterion for the onset of convection in a porous medium, with convection occurring when $Ra > 4\pi^2 \approx 39.5$. Using 'typical' TVZ fluid properties (Kissling, 2004) and adopting a temperature difference of 370°C to match the BDT temperature range used, Ra was calculated to be approximately 1140 and 11 for bounding permeabilities of 1×10^{-15} m^2 and 1×10^{-17} m^2 respectively. These are consistent with the convection and conduction-dominated regions observed in Fig 5e and Fig 5f, indicating the criterion remains relevant for the temperature range investigated. Whilst this simplified calculation supports our explanation of the simulated behaviour, it does not consider the temperature-dependent variability of density, viscosity and permeability incorporated in the numerical model. A single Ra value, therefore, would not fully capture the convective potential in a system. For this reason, the critical permeability for natural convection in this system was not explicitly calculated.

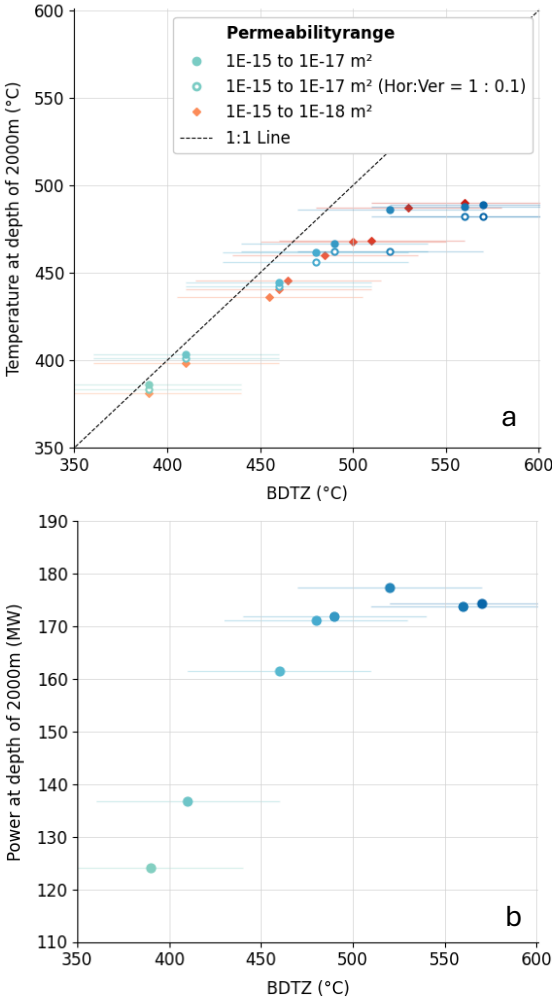

Figure 7: Sensitivity of (a) shallow geothermal temperatures and (b) convection cell power output to BDT temperature. Dashed line denotes one to one correlation, while vertical bars show the full range of the modelled temperature transition. Open symbols distinguish models with permeability anisotropy.

3.2 Effect of BDT temperature on geothermal field characteristics

Across a range of BDT temperatures, a positive correlation was observed with temperatures at 2 km depth (Fig. 7(a)). These shallow temperatures tend to be slightly below (10-20°C) the BDT midpoint for lower temperature transitions. This is evidence that shallow geothermal temperatures may provide insight into deeper permeability and thermal structure. Above an initial transition temperature of 520°C, shallow temperatures appear to be decoupled and do not increase beyond a maximum value of 490°C.

This behaviour may be an artifact of the modelling procedure, reflecting either unrealistic density or viscosity properties, or alternatively the closed vertical boundary. Further testing is needed to confirm these hypotheses.

It was found that the field power output follows a similar trend to the shallow temperature, increasing initially with

Proceedings 47th New Zealand Geothermal Workshop
11 -13 November 2025
Rotorua, New Zealand
ISSN 2703-4275

BDT temperature before levelling off below 180 MW, at the same temperature limits noted earlier. Power outputs range between 120-180 MW and are consistent with inferences for TVZ geothermal fields (Bibby et al., 1995). These results suggest that shallow measurements could be used to gain insight into the deep BDT conditions, offering a potential tool for geothermal exploration.

3.3 Model heat balance

Table 1 provides an account of the heat transfer in different regions of the model for a selection of convection cells. This analysis is useful for tracing the ultimate source of heat transported by the geothermal system.

Heat transfer in the upflow of a geothermal system is mainly convective but does contain a small amount of conduction. Heat transfer at the magma body, owing to its high temperature and hence impermeable state (Fig 5(a), (d), (g), (i)), is largely conductive. Its contribution (of about 1.65 MW to 1.8 MW) to the overall heat balance (roughly 121 to 124 MW for low BDT temperature ranges) is small owing to the relatively small volume of the intrusion when compared to the broader geothermal system.

Table 1: Heat transfer by region and mechanism. Cond.=conduction. Conv.=convection.

Perm. range (m^2)	BDT range (°C)	Region	Total (MW)	Cond. (MW)	Conv. (MW)
10^{-15} to 10^{-17}	350 to 450	Field	124	0.33	121
		Magma	1.80	1.80	0.00
		Hotplate	120	120	0.04
	520 to 620	Field	174	0.39	170
		Magma	2.98	2.98	0.00
		Hotplate	191	191	0.03
10^{-15} to 10^{-18}	340 to 410	Field	121	0.30	119
		Magma	1.65	1.65	0.00
		Hotplate	119	119	0.00
	510 to 610	Field	174	0.40	170
		Magma	2.90	2.90	0.00
		Hotplate	192	192	0.01

In contrast, the hotplate provides the bulk of the heat input into the model and thus is the primary energy source of the convection cell. The hotplate dominates due to the large effective area from which heat is transferred. In the hotplate region, heat is first conducted through the low permeability zone by a high thermal gradient. As temperature lowers and permeability increases, fluid flow increasingly becomes the dominant mechanism of heat transfer.

4. DISCUSSION AND CONCLUSIONS

The models investigated support the interpretation that shallow geothermal temperatures (~2 km depth) are sensitive to, and potentially constrain, the limiting temperature of large-scale rock-hosted fluid flow (Fig. 7(a)). One implication is that the differences in the maximum geothermal temperatures observed in distinct provinces, such as the 340°C in New Zealand, 405°C at mid-ocean ridges (Von Damm et al., 2003; Ingebritsen et al., 2010), and 450°C in Iceland, may in part be influenced by the particular

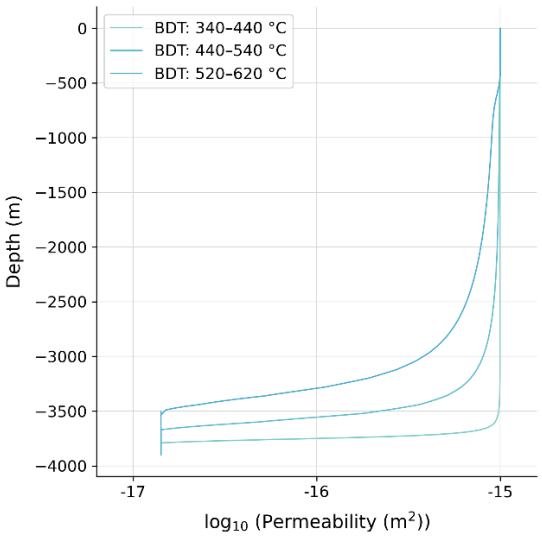

Figure 8: Permeability drop above magma chamber given a low BDT temperature range.

characteristics of those settings. A range of factors may contribute, including the rifting rate which may play a role in permeability renewal, the presence of stalled, shallow magma bodies, and the texture and/or composition of the rocks.

However, as there is some variation in field temperatures in all geothermal provinces, other local factors must also play a role. Hayba and Ingebritsen (1997) showed that, for a fixed BDT temperature, higher crustal permeabilities resulted in lower temperatures in the shallow depths of geothermal systems. The highest temperature geothermal systems occurred for host rock permeability of approximately 10^{-15} m^2, which is the value used for simulations in this work. At higher permeability, the increased velocity of convective fluids meant less time in the vicinity of high magmatic temperatures and hence lower overall fluid temperature.

Of particular interest for prospecting supercritical geothermal resources is whether there exists sufficient permeability to extract the resource. This is the case for some Iceland wells but not universally, as the examples of Larderello and Kakkonda demonstrate. The thermal models in the present work suggest that if deep circulation within the TVZ was indeed encountering temperatures higher than 400°C, then evidence of this might be reasonably expected at currently

Proceedings 47th New Zealand Geothermal Workshop
11 -13 November 2025
Rotorua, New Zealand
ISSN 2703-4275

drilled depths in developed fields, in the form of much higher temperatures. If drilling to supercritical conditions does not uncover economic permeability, then consideration would need to be given to how it might be created through stimulation. However, further improvements to the model are needed to determine the robustness of this hypothesis.

The next steps to improve this modelling include an equation of state that better aligns with the IAPWS standard to supercritical conditions. While the current model captures temperature driven buoyancy, its deviation at higher temperature might influence the upflow velocity and hence estimated power output. More detailed permeability models that take into account confining pressure and porosity, alongside temperature, would provide a more detailed understanding of permeability loss. Finally, transient simulations are likely required as convection is expected to be unstable and would also enable exploration of higher crustal permeability values.

REFERENCES

Bibby, H. M., Caldwell, T. G., Davey, F. J., & Webb, T. H. (1995). Geophysical evidence on the structure of the Taupo Volcanic Zone and its hydrothermal circulation. *Journal of Volcanology and Geothermal Research*, *68*(1-3), 29-58.

Bryan, C. J., Sherburn, S., Bibby, H. M., Bannister, S. C., & Hurst, A. W. (1999). Shallow seismicity of the central Taupo Volcanic Zone, New Zealand: its distribution and nature. *New Zealand Journal of Geology and Geophysics*, *42*(4), 533-542.

Couston, L. A., Nandaha, J., & Favier, B. (2022). Competition between Rayleigh–Bénard and horizontal convection. *Journal of Fluid Mechanics, 947*, A13.

Dempsey, D. E., Simmons, S. F., Archer, R. A., & Rowland, J. V. (2012a). Delineation of catchment zones of geothermal systems in large-scale rifted settings. *Journal of Geophysical Research: Solid Earth, 117*(B10).

Dempsey, D. E., Rowland, J. V., Zyvoloski, G. A., & Archer, R. A. (2012b). Modeling the effects of silica deposition and fault rupture on natural geothermal systems. *Journal of Geophysical Research: Solid Earth*, *117*(B5).

Fournier, R. O. (1999). Hydrothermal processes related to movement of fluid from plastic into brittle rock in the magmatic-epithermal environment. *Economic Geology*, *94*(8), 1193-1211.

Friðleifsson, G. Ó., Pálsson, B., Stefánsson, B., Albertsson, A., Gíslason, Þ., Gunnlaugsson, E., Thorsteinsson, H. H., Ketilsson, J., Sæther, S., Sörlie, C., Elders, W. A., & Zierenberg, R. A. (2020). The IDDP success story – Highlights. World Geothermal Congress 2020. https://www.worldgeothermal.org/pdf/IGAstandard/WGC/2020//37000.pdf

Hayba, D. O., & Ingebritsen, S. E. (1997). Multiphase groundwater flow near cooling plutons. *Journal of Geophysical Research: Solid Earth, 102*(B6), 12235-12252.

Hanano, M. (2004). Contribution of fractures to formation and production of geothermal resources. *Renewable and Sustainable Energy Reviews, 8*(3), 223-236.

Henneberger, R. C., & Browne, P. R. L. (1988). Hydrothermal alteration and evolution of the Ohakuri hydrothermal system, Taupo Volcanic Zone, New Zealand. *Journal of Volcanology and Geothermal Research, 34*(3-4), 211-231.

Ikeuchi, K., Doi, N., Sakagawa, Y., Kamenosono, H., & Uchida, T. (1998). High-temperature measurements in well WD-1a and the thermal structure of the Kakkonda geothermal system, Japan. *Geothermics, 27*(5-6), 591-607.

Ingebritsen, S. E., Geiger, S., Hurwitz, S., Driesner, T. (2010). Numerical simulation of magmatic hydrothermal systems. *Reviews of Geophysics*, *48*. doi: 8755-1209/10/2009RG000287.

Kissling, W. M. (2004). *Deep hydrology of the geothermal systems in the Taupo Volcanic Zone, New Zealand* (Doctoral dissertation, ResearchSpace@ Auckland).Kissling, W. M., Ellis, S., Barker, S. J., & Caldwell, T. G. (2024). A source-to-surface model of heat and fluid transport in the Taupō Rift, New Zealand. *Journal of Volcanology and Geothermal Research, 446*, 107995.

Manning, C. E., & Ingebritsen, S. E. (1999). Permeability of the continental crust: Implications of geothermal data and metamorphic systems. *Reviews of Geophysics*, *37*(1), 127-150.

Magro, G., Droghieri, E., & Gherardi, F. (2019). Drilling super-hot horizons of the Larderello geothermal field: Insights from noble gases. In *E3S Web of Conferences* (Vol. 98, p. 12012). EDP Sciences.

McNabb, A. (1975), Geothermal physics, Appl. Math. Tech. Rep., 32, Dep. of Sci. and Indust. Res., Lower Hutt, N. Z.

McNamara, D. D., Sewell, S., Buscarlet, E., & Wallis, I. C. (2016). A review of the Rotokawa geothermal field, New Zealand. *Geothermics*, *59*, 281-293.

Meyer, G. G., Shahin, G., Cordonnier, B., & Violay, M. (2024). Permeability partitioning through the brittle-to-ductile transition and its implications for supercritical geothermal reservoirs. *Nature Communications*, *15*(1), 7753.

Micklethwaite, S., & Cox, S. F. (2004). Fault-segment rupture, aftershock-zone fluid flow, and mineralization. *Geology, 32*(9), 813-816.

Mordensky, S. P., Heap, M. J., Kennedy, B. M., Gilg, H. A., Villeneuve, M. C., Farquharson, J. I., & Gravley, D. M. (2019). Influence of alteration on the mechanical behaviour and failure mode of andesite: implications for shallow seismicity and volcano monitoring. *Bulletin of Volcanology, 81*, 1-12.

Rowland, J. V., Wilson, C. J., & Gravley, D. M. (2010). Spatial and temporal variations in magma-assisted rifting, Taupo Volcanic Zone, New Zealand. *Journal of Volcanology and Geothermal Research, 190*(1-2), 89-108.

ISSN 2703-4275

Scholz, C. H. (1988). The brittle-plastic transition and the depth of seismic faulting. *Geologische Rundschau, 77*, 319-328.

Scott, S., Driesner, T., & Weis, P. (2016). The thermal structure and temporal evolution of high-enthalpy geothermal systems. *Geothermics*, *62*, 33-47.

Sewell, S. M., Addison, S. J., Hernandez, D., Azwar, L., & Barnes, M. L. (2015). Rotokawa conceptual model update 5 years after commissioning of the 138 MWe NAP plant. In Proc. NZ Geothermal Workshop.

Sibson, R. H. (1996). Structural permeability of fluid-driven fault-fracture meshes. *Journal of Structural geology*, *18*(8), 1031-1042.

Townend, J., & Zoback, M. D. (2000). How faulting keeps the crust strong. *Geology*, *28*(5), 399-402.

Villeneuve, M. C., Jones, T. P., Heap, M. J., Kennedy, B. M., Cole, J. W., & Siratovich, P. A. (2024). Physical and mechanical depth relationships of rocks from the Rotokawa Geothermal Reservoir, Taupō Volcanic Zone, New Zealand. *New Zealand Journal of Geology and Geophysics*, 1-19.

Violay, M., Gibert, B., Mainprice, D., Evans, B., Dautria, J. M., Azais, P., & Pezard, P. (2012). An experimental study of the brittle-ductile transition of basalt at oceanic crust pressure and temperature conditions. *Journal of Geophysical Research: Solid Earth*, *117*(B3).

Von Damm, K. L., Lilley, M. D., Shanks, W. C., Brockington, M., Bray, A. M., O'Grady, K. M., Olson, E., Graham, A., and Proskurowski, G. (2003). Extraordinary phase separation and segregation in vent fluids from the southern East Pacific Rise, *Earth Planet. Sci. Lett.*, 206, 365–378, doi:10.1016/S0012-821X(02)01081-6.

Watanabe, N., Numakura, T., Sakaguchi, K., Saishu, H., Okamoto, A., Ingebritsen, S. E., & Tsuchiya, N. (2017). Potentially exploitable supercritical geothermal resources in the ductile crust. *Nature Geoscience*, *10*(2), 140-144.

Weir, G. J. (2009). A mathematical model of rainfall-controlled geothermal fields. *Transport in porous media*, *77*(2), 323-334.

ISSN 2703-4275